

FEEDBACK FROM SUPERCRITICAL DISK ACCRETION FLOWS: TWO-DIMENSIONAL RADIATION-HYDRODYNAMIC SIMULATIONS OF STABLE AND UNSTABLE DISKS WITH RADIATIVELY DRIVEN OUTFLOWS

K. OHSUGA

Department of Physics, Rikkyo University, Toshimaku, Tokyo 171-8501, Japan
 Received 2006 September 19; accepted 2006 December 22

ABSTRACT

The supercritical disk accretion flow with radiatively driven outflows is studied based on two-dimensional radiation-hydrodynamic simulations for a wide range of the mass input rate, \dot{M}_{input} , which is the mass supplied from the outer region to the disk per unit time. The α -prescription is adopted for the viscosity. We employ $\alpha = 0.5$, as well as $\alpha = 0.1$, for $\dot{M}_{\text{input}} \geq 3 \times 10^2 L_E/c^2$ and only $\alpha = 0.5$ for $\dot{M}_{\text{input}} \leq 10^2 L_E/c^2$, where L_E is the Eddington luminosity and c is the speed of light. The quasi-steady disk and radiatively driven outflows form in the case in which the mass input rate highly exceeds the critical rate, $\dot{M}_{\text{input}} > 3 \times 10^2 L_E/c^2$. Then, the disk luminosity, as well as the kinetic energy output rate by the outflow, exceeds the Eddington luminosity. The moderately supercritical disk, $\dot{M}_{\text{input}} \sim 10 - 10^2 L_E/c^2$, exhibits limit-cycle oscillations. The disk luminosity goes up and down across the Eddington luminosity, and the radiatively driven outflows intermittently appear. The time-averaged mass, momentum, and kinetic energy output rates by the outflow, as well as the disk luminosity, increase with an increase of the mass input rate, $\propto \dot{M}_{\text{input}}^{0.7}$ for $\alpha = 0.5$ and $\propto \dot{M}_{\text{input}}^{0.4} - \dot{M}_{\text{input}}^{0.6}$ for $\alpha = 0.1$. Our numerical simulations show that the radiatively driven outflow model for the correlation between black hole mass and bulge velocity dispersion proposed by Silk & Rees and King is successful if $\dot{M}_{\text{input}} c^2/L_E \sim$ a few 10 ($\alpha = 0.5$) or \gtrsim a few ($\alpha = 0.1$).

Subject headings: accretion, accretion disks — black hole physics — galaxies: nuclei — hydrodynamics — radiative transfer

1. INTRODUCTION

The evolution of supermassive black holes (BHs) and their host galaxies is a major topic of current interest. The observations of high-redshift quasars showed that the supermassive BHs had formed in the early universe (Becker et al. 2001; Fan et al. 2001; Shields et al. 2006). It has been reported that the gas accretion is a significant process for evolution of the supermassive BHs (Yu & Tremaine 2002). If the supercritical accretion (the mass accretion rate exceeds the critical rate, L_E/c^2 , where L_E is the Eddington luminosity and c is the speed of light) is possible, a growth timescale of BHs can be much shorter than the Eddington timescale. Thus, the supercritical accretion might resolve the problem of the formation of supermassive BHs.

The supercritical accretion onto the central BH is also thought to play important roles for the evolution of their host galaxies. It has been suggested that the correlation between the velocity dispersion of the bulge stars (σ_*) and the BH mass ($M_{\text{BH}}-\sigma_*$ relation; Gebhardt et al. 2000; Ferrarese & Merritt 2000; Greene & Ho 2006), which implies that there is some physical link between the evolution of the BHs and the host galaxies, is established by the feedback from the supercritical accretion flows.

King (2003) suggested that the strong outflow from the supercritical accretion flow regulates the evolution of the supermassive BH and its host galaxy, leading to the $M_{\text{BH}}-\sigma_*$ relation (see also Silk & Rees 1998). However, the momentum and kinetic energy output rates by the outflow were assumed without being carefully treated, even though they are significant physical quantities in this scenario.

Umemura (2001) suggested that the $M_{\text{BH}}-\sigma_*$ relation is built up by mass accretion onto the galactic center via the radiation drag (see also Kawakatu & Umemura 2002). Since mass accretion is caused by the stellar radiation of the bulge stars, the BH

mass is correlated with the bulge mass. Although the mass accretion rate exceeds the critical rate in this mechanism, the feedback from the supercritical accretion is not taken into consideration.

Although the standard disk model, which was proposed by Shakura & Sunyaev (1973), elucidates the fundamental properties of luminous compact objects, it breaks down in the supercritical accretion regime. In this case, a large part of the photons generated inside the disk via the viscous process is advected inward and swallowed by the BH with accreting matter. This is the so-called photon trapping in the disk accretion flows (Ohsuga et al. 2002, 2003; Shimura & Manmoto 2003). The radiation pressure becomes dominant over the gas pressure and drives the radiatively driven outflows. The circular motion, as well as the convection, occurs in the disk. They are basically multidimensional effects. These effects are not correctly treated in the slim disk (Abramowicz et al. 1988), since it is a radially one-dimensional model.

The two-dimensional radiation hydrodynamic (RHD) simulations of the supercritical disk accretion flows around the BHs were initiated by Eggum et al. (1988) and improved by Okuda (2002). Ohsuga et al. (2005) for the first time succeeded in reproducing the quasi-steady structure of the supercritical disk accretion flows. Ohsuga (2006) performed the numerical simulations of the unstable disks with the moderately supercritical accretion rate. However, the outflow from the supercritical accretion flow is poorly understood. Whereas the radiatively driven outflow has been extensively studied by many researchers (e.g., Bisnovatyi-Kogan & Blinnikov 1977; Watarai & Fukue 1999), they treat the disk as an external radiation source and do not solve the radiation transfer.

In this paper, by performing two-dimensional RHD simulations of stable and unstable disks, we report the feedback (mass, momentum, and energy output rates) from the supercritical disk

accretion flows around BHs for a wide range of the mass input rate, which is the mass supplied from the outer region to the disk per unit time.

2. BASIC EQUATIONS AND NUMERICAL METHOD

Basic equations and our numerical methods are described in detail in Ohsuga et al. (2005) and Ohsuga (2006). The set of RHD equations including the viscosity term is solved by an explicit-implicit finite-difference scheme on the Eulerian grids. Here, we use spherical polar coordinates (r, θ, φ) , where r is the radial distance, θ is the polar angle, and φ is the azimuthal angle. The origin is set at a central BH. Since we assume axisymmetry (i.e., $\partial/\partial\varphi = 0$), as well as reflection symmetry relative to the equatorial plane (with $\theta = \pi/2$), the computational domain can be restricted to one quadrant of the meridional plane. The domain consists of spherical shells of $3r_s \leq r \leq 500r_s$ and $0 \leq \theta \leq \pi/2$ and is divided into 96×96 grid cells, where r_s is the Schwarzschild radius. We describe the gravitational field of the BH in terms of pseudo-Newtonian hydrodynamics, in which the gravitational potential is given by $-GM_{\text{BH}}/(r - r_s)$, as was introduced by Paczynsky & Wiita (1980). The flow is assumed to be non-self-gravitating. The basic equations are the continuity equation,

$$\frac{\partial \rho}{\partial t} + \nabla \cdot (\rho \mathbf{v}) = 0, \quad (1)$$

the equations of motion,

$$\begin{aligned} \frac{\partial(\rho v_r)}{\partial t} + \nabla \cdot (\rho v_r \mathbf{v}) \\ = -\frac{\partial p}{\partial r} + \rho \left[\frac{v_\theta^2}{r} + \frac{v_\varphi^2}{r} - \frac{GM_{\text{BH}}}{(r - r_s)^2} \right] + f_r + q_r, \end{aligned} \quad (2)$$

$$\frac{\partial(\rho v_\theta)}{\partial t} + \nabla \cdot (\rho v_\theta \mathbf{v}) = -\frac{\partial p}{\partial \theta} + \rho v_\varphi^2 \cot \theta + r f_\theta + r q_\theta, \quad (3)$$

$$\frac{\partial[\rho r \sin \theta (v_\varphi)]}{\partial t} + \nabla \cdot [\rho r \sin \theta (v_\varphi \mathbf{v})] = r \sin \theta (q_\varphi), \quad (4)$$

the energy equation of the gas,

$$\frac{\partial e}{\partial t} + \nabla \cdot (e \mathbf{v}) = -p \nabla \cdot \mathbf{v} - 4\pi \kappa B + c\kappa E_0 + \Phi_{\text{vis}}, \quad (5)$$

and the energy equation of the radiation,

$$\frac{\partial E_0}{\partial t} + \nabla \cdot (E_0 \mathbf{v}) = -\nabla \cdot \mathbf{F}_0 - \nabla \mathbf{v} : \mathbf{P}_0 + 4\pi \kappa B - c\kappa E_0, \quad (6)$$

where ρ is the mass density, $\mathbf{v} = (v_r, v_\theta, v_\varphi)$ is the velocity, p is the gas pressure, e is the internal energy density of the gas, B is the blackbody intensity, E_0 is the radiation energy density, \mathbf{F}_0 is the radiative flux, \mathbf{P}_0 is the radiation pressure tensor, κ is the absorption opacity, $\mathbf{q} = (q_r, q_\theta, q_\varphi)$ is the viscous force, and Φ_{vis} is the viscous dissipative function.

The radiation force $\mathbf{f}_{\text{rad}} = (f_r, f_\theta)$ is given by

$$\mathbf{f}_{\text{rad}} = \frac{\chi}{c} \mathbf{F}_0, \quad (7)$$

where $\chi (= \kappa + \rho \sigma_T / m_p)$ is the total opacity with σ_T being the Thomson scattering cross section and m_p being the proton mass. For the absorption opacity, we consider the free-free absorption and the bound-free absorption for solar metallicity (Hayashi et al. 1962; Rybicki & Lightman 1979). In the present study, the outflow is mainly accelerated by the radiation force on the Thomson scattering, although the radiation force on the free-free and bound-free absorption is also taken into consideration.

As the equation of state, we use

$$p = (\gamma - 1)e, \quad (8)$$

where γ is the specific heat ratio. The temperature of the gas, T , can then be calculated from

$$p = \frac{\rho k_B T}{\mu m_p}, \quad (9)$$

where k_B is the Boltzmann constant and μ is the mean molecular weight.

The radiative flux and the radiation stress tensor are solved under the flux-limited diffusion approximation (Levermore & Pomraning 1981), so that they are expressed in terms of the radiation energy density (Turner & Stone 2001). It gives correct relations in the optically thick diffusion limit and optically thin streaming limit, respectively.

In this paper we assume that only the $r\varphi$ -component of the viscous stress tensor is nonzero, leading $q_r = q_\theta = 0$. This component plays important roles for the transport of the angular momentum and the heating of the disk plasma. In our form, it is proportional to αp_{total} in the optically thick limit and αp in the optically thin limit, where α and p_{total} are the viscosity parameter and the total pressure, respectively. Our viscosity model is basically the same as the α -prescription of the viscosity proposed by Shakura & Sunyaev (1973).

We start the calculations with a hot, rarefied, optically thin atmosphere. There is no cold dense disk initially. We assume that matter is continuously injected into the computational domain through the outer disk boundary ($r = 500r_s$, $0.45\pi \leq \theta \leq 0.5\pi$). The injected matter is supposed to have a specific angular momentum corresponding to the Keplerian angular momentum at $r = 100r_s$. We set the injected mass accretion rate (mass input rate, \dot{M}_{input}) so as to be constant at the boundary.

Throughout the present study we assume $M_{\text{BH}} = 10 M_\odot$, $\gamma = 5/3$, and $\mu = 0.5$. The α -parameter is set to be 0.5 and 0.1. The time step is $\sim 3 \times 10^{-6}$ s, which is determined by $\min[\Delta r/c, r\Delta\theta/c]$, where Δr and $\Delta\theta$ are the cell sizes in the radial and polar directions, respectively.

3. RESULTS

3.1. Highly Supercritical Case

In Figure 1 we plot the time evolution of the mass accretion rate onto the BH \dot{M}_{BH} (black line, top), the luminosity L_{rad} (black line, bottom), and the mass and kinetic energy output rates \dot{M}_{out} (red line) and L_{kin} (blue line) for $\dot{M}_{\text{input}} = 10^3 L_E / c^2$, where the viscosity parameter is set to be 0.5. The luminosity is evaluated by integrating the radiative flux at the outer boundary. It almost equals the luminosity of the disk. The mass and kinetic energy output rates indicate the mass and kinetic energy ejected through the outer boundary per unit time by the outflow of $v_r > v_{\text{esc}}$, where v_{esc} is the escape velocity.

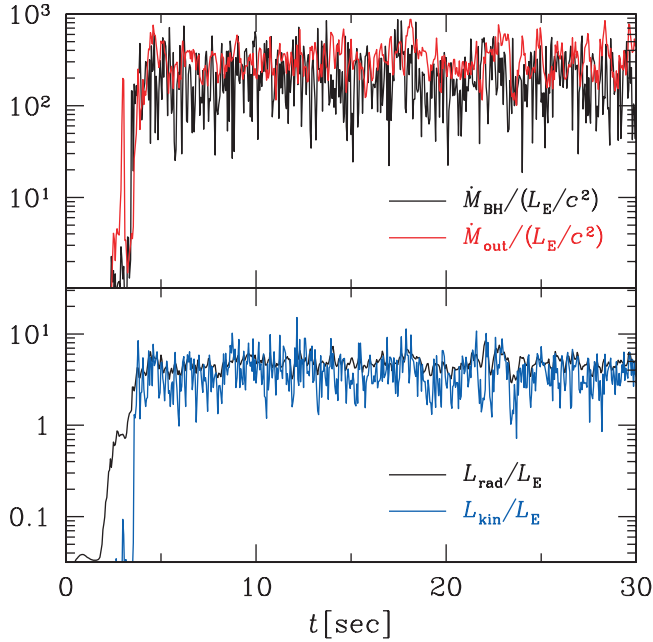


FIG. 1.—Time evolution of the mass accretion rate onto the BH (black line, top), the mass output rate (red line), the luminosity (black line, bottom), and kinetic energy output rate (blue line) for $\dot{M}_{\text{input}} = 10^3 L_E/c^2$. The viscosity parameter α is set to be 0.5.

Since the matter injected from the outer disk boundary has angular momentum, it accumulates in the computational domain without accreting onto the BH in the early evolutionary phase ($t \lesssim 3$ s). The matter starts to accrete onto the BH at $t \sim 3$ s. This critical time roughly coincides with the viscous timescale (see eq. [2] in Ohsuga et al. [2005]). All the quantities stay nearly constant when $t \gtrsim 3$ s. The total mass contained within the computational domain is also constant in this phase. Thus, we conclude that the flow is quasi-steady in this phase. The radiation-pressure-dominated thick disk forms, and the radiatively driven outflows appear above and below the disk. The quasi-steady structure is similar to that in Ohsuga et al. (2005), although they employ $\alpha = 0.1$.

As shown in Figure 1, the mass accretion rate is about 2 orders of magnitude larger than the critical rate, and the luminosity stays around $4.8 L_E$ in the quasi-steady state. We also find that the strong and quasi-steady outflow is generated. The mass output rate is comparable to the mass accretion rate. The kinetic energy output rate exceeds the Eddington luminosity, whereas it is slightly smaller than the luminosity. The energy conversion efficiency, $(L_{\text{rad}} + L_{\text{kin}})/\dot{M}_{\text{BH}}c^2$, is much smaller than the prediction of the standard disk, ~ 0.1 . This is because a large amount of photons generated inside the disk are swallowed by the BH without being radiated away by the photon trapping.

3.2. Moderately Supercritical Case

Next we show the time evolution in the case in which the mass input rate moderately exceeds the critical rate in Figure 2. Here, we set the mass input rate to be $10^2 L_E/c^2$ and the viscosity parameter to be 0.5. In this case, the mass accretion rate drastically varies, although the matter is continuously injected into the computational domain at a constant rate. The mass accretion rate suddenly rises from $\sim 0.3 L_E/c^2$ to $\sim 300 L_E/c^2$, and it decays after 10 s. Such time variation of the mass accretion rate occurs

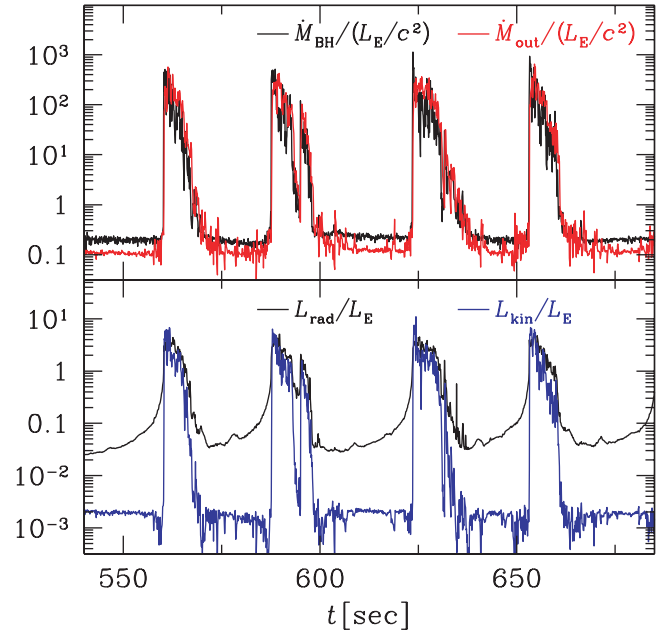


FIG. 2.—Same as Fig. 1, but for $\dot{M}_{\text{input}} = 10^2 L_E/c^2$.

at intervals of ~ 60 s and triggers off the luminosity oscillations. The luminosity is around $0.03 L_E$ in the low-luminosity state and $3 L_E$ in the high-luminosity state. The photon trapping reduces the luminosity in the high state.

Such disk oscillations are induced by the disk instability in the radiation-pressure-dominated region. The disk theory predicts that the radiation-pressure-dominated disk is unstable if the radiative cooling is dominant over the advective cooling (Lightman & Eardley 1974; Shibasaki & Hōshi 1975; Kato et al. 1998). Since the advective cooling becomes the main cooling process when the mass accretion rate is much higher than the critical rate, the disk with a highly supercritical accretion rate is stabilized. In contrast, the moderately supercritical disk exhibits limit-cycle oscillations.

In Figure 2 we also find that the strong outflow appears only in the high-luminosity state. In this state, the mass output rate is about 2 orders of magnitude larger than the critical rate. The kinetic energy output rate exceeds the Eddington luminosity and is comparable to the luminosity. In contrast, it is found that L_{kin} is much smaller than L_{rad} in the low-luminosity state. It implies that the matter is not effectively accelerated by the radiation force when the disk shines at sub-Eddington luminosity. The radiatively driven outflows are intermittently produced in the case in which the mass input rate moderately exceeds the critical rate.

The mass ejected from the computational domain per unit time (sum of the mass accretion rate onto the BH and the mass ejection rate through the outer boundary) almost equals the mass input rate on average. Thus, simulated limit-cycle behavior is not a transient phenomenon. It would continue as long as the mass input rate does not change so much. Here we note that such a balance between mass input and ejection rates is for the first time reproduced in the present simulations, since our integration time is much longer than that in Ohsuga (2006) and the relatively large viscosity parameter is employed.

Our simulations show that the disk is also unstable and exhibits the limit-cycle oscillations in the case of $\dot{M}_{\text{input}} = 10 L_E/c^2$ (see Fig. 3). As compared with the case of $\dot{M}_{\text{input}} = 10^2 L_E/c^2$, the

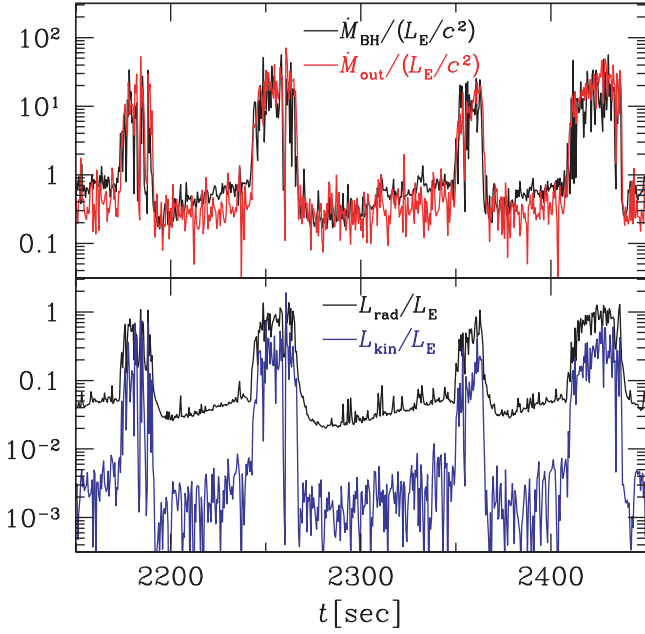


FIG. 3.—Same as Fig. 1, but for $\dot{M}_{\text{input}} = 10L_E/c^2$.

bursting behavior is not remarkable. The luminosity, as well as the kinetic energy output rate, is comparable to or less than the Eddington luminosity even in the high-luminosity state.

3.3. Feedback

Based on the results of our numerical simulations for $\alpha = 0.5$, we represent in Figure 4 the time-averaged mass accretion rate onto the BH (*triangles*), luminosity (*squares*), mass output rate (*red circles*), kinetic energy output rate (*blue circles*), and momentum output rate $\dot{M}_{\text{out}}v$ (*green circles*) as functions of the

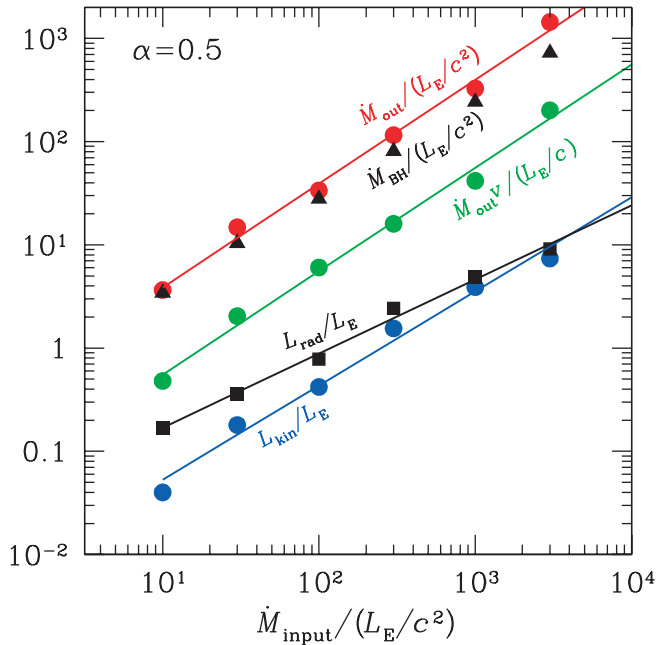


FIG. 4.—Time-averaged mass output rate (*red circles*), the kinetic energy output rate (*blue circles*), and the momentum output rate (*green circles*) by the outflow for $\alpha = 0.5$. The mass accretion rate onto the BH and the luminosity are plotted with triangles and squares. Red, blue, green, and black lines represent the fitting formulae of equations (10)–(13), respectively.

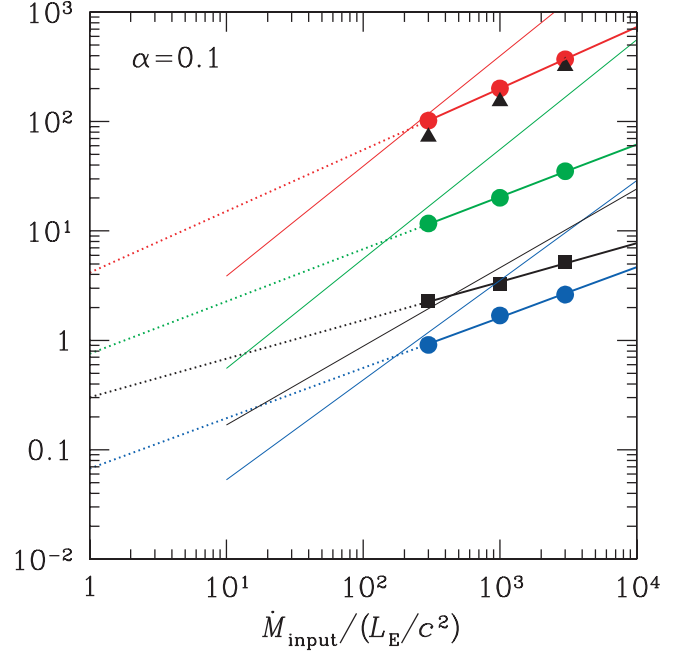


FIG. 5.—Same as Fig. 4, but for $\alpha = 0.1$. Thick solid lines represent the fitting formulae of equation (14)–(17). They are extended onto the small mass input regime (*dotted lines*). The fitting formulae for $\alpha = 0.5$ are plotted by thin lines.

mass input rate. Here, the momentum output rate means the radial component of the momentum carried out of the computational domain per unit time through the outer boundary by the outflow of $v_r > v_{\text{esc}}$. The disks with $\dot{M}_{\text{input}} > 3 \times 10^2 L_E/c^2$ are stable. In contrast, the disks exhibit the limit-cycle behavior in the case of $\dot{M}_{\text{input}} = 10\text{--}10^2 L_E/c^2$.

We find that all quantities monotonously rise with an increase of \dot{M}_{input} . We present simple fitting formulae with the least-squares method for our numerical results; feedback from the supercritical disk accretion flows in the case of $\alpha = 0.5$ are given by

$$\log\left(\frac{\dot{M}_{\text{out}}}{L_E/c^2}\right) = \log\left(\frac{\dot{M}_{\text{input}}c^2}{L_E}\right) - 0.42, \quad (10)$$

$$\log\left(\frac{L_{\text{kin}}}{L_E}\right) = 0.91 \log\left(\frac{\dot{M}_{\text{input}}c^2}{L_E}\right) - 2.2, \quad (11)$$

$$\log\left(\frac{\dot{M}_{\text{out}}v}{L_E/c}\right) = \log\left(\frac{\dot{M}_{\text{input}}c^2}{L_E}\right) - 1.3, \quad (12)$$

$$\log\left(\frac{L_{\text{rad}}}{L_E}\right) = 0.72 \log\left(\frac{\dot{M}_{\text{input}}c^2}{L_E}\right) - 1.5. \quad (13)$$

These fitting formulae are also plotted by red, blue, green, and black lines in Figure 4, respectively. Here, it is noted that they are valid only in the supercritical accretion regime. If the mass input rate is comparable to or less than the critical rate, the standard disk, which is not accompanied by the outflow, would form.

Whereas Figure 4 shows the feedback effects in the case of $\alpha = 0.5$ as functions of the mass input rate, they are sensitive to the viscosity parameter. In Figure 5 we show the resulting feedback effects for $\alpha = 0.1$. Here, there are no results for $\dot{M}_{\text{input}} < 10^2 L_E/c^2$. We need to consume much time in the numerical simulations for a small mass input rate because of the

long viscous timescale. In this figure, thick solid lines represent the fitting formulae for $\alpha = 0.1$. They are

$$\log\left(\frac{\dot{M}_{\text{out}}}{L_E/c^2}\right) = 0.56 \log\left(\frac{\dot{M}_{\text{input}} c^2}{L_E}\right) + 0.62, \quad (14)$$

$$\log\left(\frac{L_{\text{kin}}}{L_E}\right) = 0.46 \log\left(\frac{\dot{M}_{\text{input}} c^2}{L_E}\right) - 1.2, \quad (15)$$

$$\log\left(\frac{\dot{M}_{\text{out}} v}{L_E/c}\right) = 0.48 \log\left(\frac{\dot{M}_{\text{input}} c^2}{L_E}\right) - 0.12, \quad (16)$$

$$\log\left(\frac{L_{\text{rad}}}{L_E}\right) = 0.35 \log\left(\frac{\dot{M}_{\text{input}} c^2}{L_E}\right) - 0.52. \quad (17)$$

Although they are derived based on the results for $\dot{M}_{\text{input}} > 3 \times 10^2 L_E/c^2$, we extend them onto the small mass input regime (*dotted lines*). The fitting formulae for $\alpha = 0.5$ are also plotted by thin lines. As shown in this figure, we find that feedback effects are more sensitive to the mass input rate for $\alpha = 0.5$ than for $\alpha = 0.1$. It is also found that the fitting formulae for the two cases intersect around $\dot{M}_{\text{input}} = 3 \times 10^2 L_E/c^2$.

Since King (2003) proposed that the $M_{\text{BH}}-\sigma_*$ relation is established via radiatively driven outflow from the supercritical accretion flow onto the supermassive BH in the galactic center. The momentum output rate $\dot{M}_{\text{out}} v$ is assumed to be $\sim L_E/c$ in their model. Thus, our results imply that their outflow model is successful as long as the normalized mass input rate, $\dot{M}_{\text{input}} c^2/L_E$, is a few tens in the case of $\alpha = 0.5$ (see the green line in Fig. 4). In the case of $\alpha = 0.1$, the fitting formula for the momentum output rate predicts that the King model is successful for $\dot{M}_{\text{input}} c^2/L_E \sim$ a few (see the green dotted line in Fig. 5). However, we should note that the fitting formulae for $\alpha = 0.1$ are derived based on the results for high mass input rate, and there are no numerical results for small mass input rate. The fitting formulae might overestimate the power of the radiatively driven outflow around $\dot{M}_{\text{input}} \sim L_E/c^2$. This is because the radiation force, which is comparable to the gravity, cannot efficiently accelerate the outflow. In this case, the normalized mass input rate for establishment of the $M_{\text{BH}}-\sigma_*$ relation would shift toward the higher \dot{M}_{input} side. We need further studies to understand the α -dependence in detail.

4. DISCUSSION

4.1. Formation of Supermassive Black Holes

Our simulations show that the highly supercritical disk is stable and the moderately supercritical disk exhibits limit-cycle oscillations. The physical mechanism for mass supply from the host galaxy onto the galactic center is one of the most hotly debated issues. Although its time evolution is not understood yet, the normalized mass input rate ($\propto \dot{M}_{\text{input}}/M_{\text{BH}}$) would gradually decrease as the seed BH grows into the supermassive BH. Thus, our results imply that the seed BH grows via the supercritical disk accretion flow in the early phase, and subsequently, the BH accretion disk evolves into the subcritical phase by way of the oscillation phase. The growth timescale via supercritical accretion is $M_{\text{BH}}/\dot{M}_{\text{BH}} = 4.5 \times 10^6 (\dot{M}_{\text{BH}} c^2 / 10^2 L_E)^{-1}$ yr.

Here, we note that our results would not change that much even if we employ a large BH mass ($M_{\text{BH}} \gg 10 M_\odot$), since the radiation force on the Thomson scattering mainly supports the disk and accelerates the outflow in our simulations. The gas density decreases with an increase of the BH mass, $\rho \propto M_{\text{BH}}^{-1}$, on the condition that the normalized mass input rate is kept constant.

Hence, the radiation force on the Thomson scattering ($\propto \rho$) is dominant over that on the bound-free and free-free absorptions ($\propto \rho^2$) even in the case of massive BHs.

Umemura (2001) suggested the model for quasar formation by which the mass is supplied onto the galactic center via the radiation drag, forming the supermassive BH in $\sim 10^9$ yr. Although the mass supply rate onto the galactic center highly exceeds the critical rate in their model, they assumed the accretion rate onto the BH to be the critical rate. The supercritical accretion onto the central BH would lead the emergence of quasars in the early evolutionary phase ($\ll 10^9$ yr). The radiation and radiatively driven outflow would affect the stellar evolution of the host galaxy. It is not taken into consideration in their model. Especially, if the metallicity of the gas is much smaller than the local interstellar value, it is known that the ultraviolet radiation plays important roles on the star formation activity (Hieman et al. 1997; Susa & Umemura 2006).

4.2. Outflows

The velocity of the radiatively driven outflow in our simulations is $0.1c-0.3c$. It is roughly consistent with the results from the observations of quasars. The observations of the blueshifted X-ray absorption lines have revealed that quasars eject the highly ionized matter with a velocity of $\sim 0.1c$ (Pounds et al. 2003a, 2003b; Reeves et al. 2003).

Line opacities are not taken into consideration in our simulations. The outflow would be enhanced via the radiation force on lines, unless the matter is highly ionized by strong radiation fields (Proga et al. 2000; Chelouche & Netzer 2003; Proga & Kallman 2004). The line force is thought to be one of the acceleration mechanisms of the outflows in active galactic nuclei (AGNs). The AGNs likely have powerful outflows even for $L_{\text{rad}} < L_E$.

Proga (1999) studied the disk winds driven by line force for $L_{\text{rad}} < L_E$, based on the stellar wind model given by Castor et al. (1975). They concluded that the mass output rate scales with the luminosity as $\dot{M}_{\text{out}} \propto (L_{\text{rad}}/L_E) - (L_{\text{rad}}/L_E)^{2.5}$. Our results do not deviate from their result. We derive the relations of $\dot{M}_{\text{out}} \propto (L_{\text{rad}}/L_E)^{1.4}$ from equations (10) and (13), as well as $\dot{M}_{\text{out}} \propto (L_{\text{rad}}/L_E)^{1.6}$ from equations (14) and (17). Note that the disk is treated as the source of radiation and mass without solving its structure in their work. In contrast, both the disk and the outflow are solved in our simulations. In addition, the central BH swallows a large amount of matter in our work.

The magnetic effects might also enhance the outflow. It has been reported by magnetohydrodynamic (MHD) simulations that the magnetized accretion disks produce the outflows, although these simulations focus on the radiatively inefficient accretion flow (Hawley & Balbus 2002; Kudoh et al. 2002; Kato et al. 2004).

4.3. Future Work

In this paper we investigate the feedback from the supercritical disk accretion flows around BHs as functions of the mass input rate. Although we employ merely two viscosity parameters, $\alpha = 0.5$ and 0.1 , the feedback effects might be more sensitive to the viscosity parameter than to the mass input rate. In addition, we do not present results for $\dot{M}_{\text{input}} < 10^2 L_E/c^2$ in the case of $\alpha = 0.1$. Further long integration time is required to simulate the accretion flows with a small viscosity parameter and/or a small mass input rate because of the long viscous timescale. Such numerical simulations are left as future work.

More importantly, we need radiation MHD simulations, since the source of disk viscosity is likely to be of magnetic origin

(Stone et al. 1999; Stone & Pringle 2001; Hawley et al. 2001; Machida et al. 2001). A more physical treatment of the viscosity might lead to the difference from the α -disks. Whereas local radiation MHD simulations have been performed recently (e.g., Turner et al. 2003), global simulations should be explored in future work.

5. CONCLUSIONS

By performing the two-dimensional RHD simulations, we study the feedback (mass, momentum, and energy output rates) from the supercritical disk accretion flows around BHs for the wide range of the mass input rate, $\dot{M}_{\text{input}} = 10\text{--}3 \times 10^3 L_E/c^2$. The adopted viscosity parameter, α , is 0.5 and 0.1 for $\dot{M}_{\text{input}} \geq 3 \times 10^2 L_E/c^2$ and only 0.5 for $\dot{M}_{\text{input}} \leq 10^2 L_E/c^2$. The detailed study for α -dependence is left as future work. We summarize our results as follows.

1. In the case of high mass input rate, $\dot{M}_{\text{input}} > 3 \times 10^2 L_E/c^2$, the quasi-steady disk forms, and the outflows driven by the radiation force appear above and below the disk. Both energy output rates by the radiation and the outflow exceed the Eddington luminosity.

2. The disk with moderately supercritical rate, $\dot{M}_{\text{input}} \sim 10\text{--}10^2 L_E/c^2$, exhibits limit-cycle oscillations, leading to intermittent outflows. The strong outflow is generated only in the high-

luminosity state, in which the energy output rates by the radiation and the outflow are comparable to or exceed the Eddington luminosity.

3. The time-averaged mass, momentum, and kinetic energy output rates by the outflow, as well as the disk luminosity, scale with mass input rate as $\propto \dot{M}_{\text{input}}^{0.7} - \dot{M}_{\text{input}}^{1.0}$ for $\alpha = 0.5$. In the case of $\alpha = 0.1$, we find that they are proportional to $\dot{M}_{\text{input}}^{0.4} - \dot{M}_{\text{input}}^{0.6}$.

4. Our numerical simulations show that the radiatively driven outflow model for the $M_{\text{BH}}\text{--}\sigma_*$ relation proposed by Silk & Rees (1998) and King (2003) is successful, as long as the normalized mass input rate, $\dot{M}_{\text{input}} c^2/L_E$, is around a few 10 ($\alpha = 0.5$) or a few ($\alpha = 0.1$).

We would like to thank the anonymous reviewer for many helpful suggestions, which greatly improved the original manuscript. We especially thank J. P. Ostriker, S. Mineshige, and H. Susa for useful comments and discussions. The calculations were carried out by a parallel computer at Rikkyo University and the Institute of Natural Science, Senshu University. We acknowledge a research grant from the Japan Society for the Promotion of Science (17740111).

REFERENCES

- Abramowicz, M. A., Czerny, B., Lasota, J. P., & Szuszkiewicz, E. 1988, *ApJ*, 332, 646
- Becker, R. H., et al. 2001, *AJ*, 122, 2850
- Bisnovatyi-Kogan, G. S., & Blinnikov, S. I. 1977, *A&A*, 59, 111
- Castor, J. I., Abbott, D. C., & Klein, R. I. 1975, *ApJ*, 195, 157
- Chelouche, D., & Netzer, H. 2003, *MNRAS*, 344, 223
- Eggum, G. E., Coroniti, F. V., & Katz, J. I. 1988, *ApJ*, 330, 142
- Fan, X., et al. 2001, *AJ*, 122, 2833
- Ferrarese, L., & Merritt, D. 2000, *ApJ*, 539, L9
- Gebhardt, K., et al. 2000, *ApJ*, 539, L13
- Greene, J. E., & Ho, L. C. 2006, *ApJ*, 641, L21
- Haiman, Z., Rees, M., & Loeb, A. 1997, *ApJ*, 476, 458
- Hawley, J. F., & Balbus, S. A. 2002, *ApJ*, 573, 738
- Hawley, J. F., Balbus, S. A., & Stone, J. M. 2001, *ApJ*, 554, L49
- Hayashi, C., Hoshi, R., & Sugimoto, D. 1962, *Prog. Theor. Phys. Suppl.*, 22, 1
- Kato, S., Fukue, J., & Mineshige, S. 1998, *Black-Hole Accretion Disks* (Kyoto: Kyoto Univ. Press)
- Kato, Y., Mineshige, S., & Shibata, K. 2004, *ApJ*, 605, 307
- Kawakatu, N., & Umemura, M. 2002, *MNRAS*, 329, 572
- King, A. 2003, *ApJ*, 596, L27
- Kudoh, T., Matsumoto, R., & Shibata, K. 2002, *PASJ*, 54, 267
- Levermore, C. D., & Pomraning, G. C. 1981, *ApJ*, 248, 321
- Lightman, A. P., & Eardley, D. M. 1974, *ApJ*, 187, L1
- Machida, M., Matsumoto, R., & Mineshige, S. 2001, *PASJ*, 53, L1
- Ohsuga, K. 2006, *ApJ*, 640, 923
- Ohsuga, K., Mineshige, S., Mori, M., & Umemura, M. 2002, *ApJ*, 574, 315
- Ohsuga, K., Mineshige, S., & Watarai, K. 2003, *ApJ*, 596, 429
- Ohsuga, K., Mori, M., Nakamoto, T., & Mineshige, S. 2005, *ApJ*, 628, 368
- Okuda, T. 2002, *PASJ*, 54, 253
- Paczynsky, B., & Wiita, P. J. 1980, *A&A*, 88, 23
- Pounds, K. A., King, A. R., Page, K. L., & O'Brien, P. T. 2003a, *MNRAS*, 346, 1025
- Pounds, K. A., Reeves, J. N., King, A. R., Page, K. L., O'Brien, P. T., & Turner, M. J. L. 2003b, *MNRAS*, 345, 705
- Proga, D. 1999, *MNRAS*, 304, 938
- Proga, D., & Kallman, T. R. 2004, *ApJ*, 616, 688
- Proga, D., Stone, J. M., & Kallman, T. R. 2000, *ApJ*, 543, 686
- Reeves, J. N., O'Brien, P. T., & Ward, M. J. 2003, *ApJ*, 593, L65
- Rybicki, G. B., & Lightman, A. P. 1979, *Radiative Processes in Astrophysics* (New York: Wiley)
- Shakura, N. I., & Sunyaev, R. A. 1973, *A&A*, 24, 337
- Shibasaki, N., & Hōshi, R. 1975, *Prog. Theor. Phys.*, 54, 706
- Shields, G. A., Menezes, K. L., Massart, C. A., & Vanden Bout, P. 2006, *ApJ*, 641, 683
- Shimura, T., & Manmoto, T. 2003, *MNRAS*, 338, 1013
- Silk, J., & Rees, M. J. 1998, *A&A*, 331, L1
- Stone, J. M., & Pringle, J. E. 2001, *MNRAS*, 322, 461
- Stone, J. M., Pringle, J. E., & Begelman, M. C. 1999, *MNRAS*, 310, 1002
- Susa, H., & Umemura, M. 2006, *ApJ*, 645, 93L
- Turner, N. J., & Stone, J. M. 2001, *ApJS*, 135, 95
- Turner, N. J., Stone, J. M., Krolik, J. H., & Sano, T. 2003, *ApJ*, 593, 992
- Umemura, M. 2001, *ApJ*, 560, L29
- Watarai, K., & Fukue, J. 1999, *PASJ*, 51, 725
- Yu, Q., & Tremaine, S. 2002, *MNRAS*, 335, 965